MINERALOGICAL MAGAZINE, DECEMBER 1979, VOL. 43, PP. 519-26

The nature and significance of exsolved phases in some chrome spinels from the Rhum layered intrusion

A. PUTNIS AND G. D. PRICE

Mineral Sciences Group, Department of Mineralogy and Petrology, Downing Place, Cambridge CB2 3EW

SUMMARY. Chrome spinels from seams in the Rhum layered intrusion, Inner Hebrides, generally contain very fine platelets of exsolved phases. Despite the low bulk Ti content (< 1%) of the spinel grains, analytical electron microscopy shows these platelets to be highly enriched in titanium. Electron diffraction indicates the presence of platelets of two different phases, one a magnesian ilmenite, the other a defect spinel intermediate phase. The platelets are the result of oxidation of the spinel at moderate (*c.* 600 °C) temperatures and their distribution suggests that oxygen fugacity gradients existed across some of the seams.

CHROME spinels are common accessory minerals in basic and ultrabasic igneous rocks. On initial crystallization from the magma they are generally considered to be stoichiometric with general formula AB_2O_4 where the A cations are tetrahedrally coordinated and may be Fe^{2+}, Mg^{2+}, Fe^{3+} and the octahedrally coordinated B cations may be Cr^{3+}, Al^{3+}, Ti^{4+}, Fe^{2+}, Fe^{3+}. However the changes in oxygen fugacity, f_{O_2}, which will occur during the cooling of such igneous bodies may lead to departures from stoichiometry in iron-bearing spinels, if their stability field in f_{O_2}-T space is intersected by the f_{O_2} cooling curve of the host rock. Oxidation or reduction processes may bring about such changes in stoichiometry, but in the environment we will consider here we are solely concerned with oxidation.

In order to maintain charge balance, the oxidation of Fe^{2+} to Fe^{3+} will be accompanied by the formation of cation vacancies. Except at very high temperatures such non-stoichiometry cannot be tolerated by the spinel structure and these defect spinels are metastable with respect to the exsolution of a sesquioxide phase R_2O_3. Under these conditions the equilibrium assemblage at low temperatures consists of a stoichiometric spinel phase and a rhombohedral sesquioxide phase.

The composition of the rhombohedral phase that forms depends on the composition of the spinel, the oxygen fugacity, and the temperature. For example, Turnock and Eugster (1962) have experimentally demonstrated that the oxidation of hercynite ($FeAl_2O_4$) leads to the formation of corundum and magnetite. At higher oxygen fugacities hematite may also form. Similarly the oxidation of Ti-bearing magnetites results in the 'oxidation exsolution' of ilmenite lamellae (Buddington and Lindsley, 1964).

Alternatively, at low temperatures the nucleation of a rhombohedral phase from the non-stoichiometric spinel may be kinetically impeded due to the high activation energy for the process. Under these non-equilibrium conditions an ordered or partially ordered defect spinel phase may form with a structure based on the parent spinel structure. The low temperature oxidation of magnetite is an example of such a metastable process and results in the formation of maghemite, which is a superstructure of the parent spinel phase (Lindsley, 1976).

The problem of the oxidation of chrome spinels with complex compositions has not been investigated experimentally but some data on such systems may be obtained by a study of natural oxidized assemblages. Ideally such an assemblage should involve a variation in initial spinel composition as well as oxygen fugacity. The chrome spinels that form thin seams between allivalite and peridotite layers in the Rhum layered intrusion, Inner Hebrides (Brown, 1956) provide both of these requirements.

Electron microprobe analyses of individual chrome spinel grains show a systematic variation in composition across the seams. Spinels that lie directly above or below the seams (within the peridotite or allivalite respectively) also have different compositions. These variations in composition and possible post-depositional re-equilibration reactions that cause them have been discussed by Henderson and Suddaby (1971) and Henderson (1975). The variation in oxygen fugacity arises from

© *Copyright the Mineralogical Society*

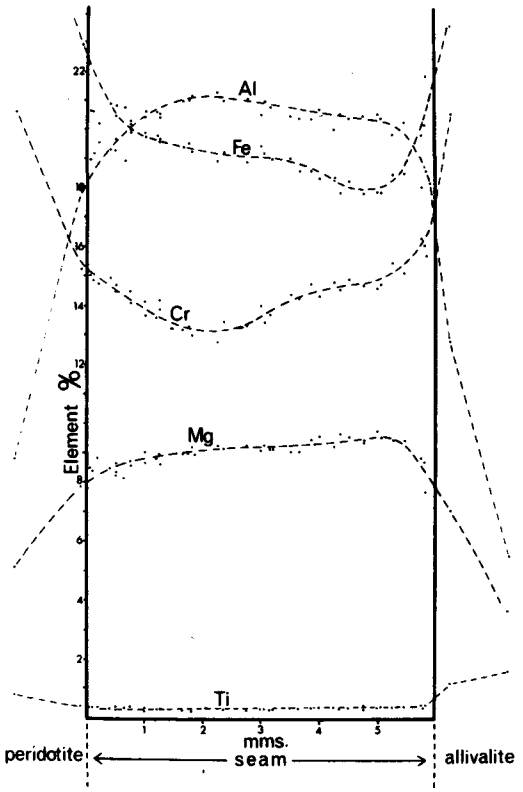

FIG. 1. Variation in chrome spinel compositions across the seam in R117. The top of the seam lies on the left.

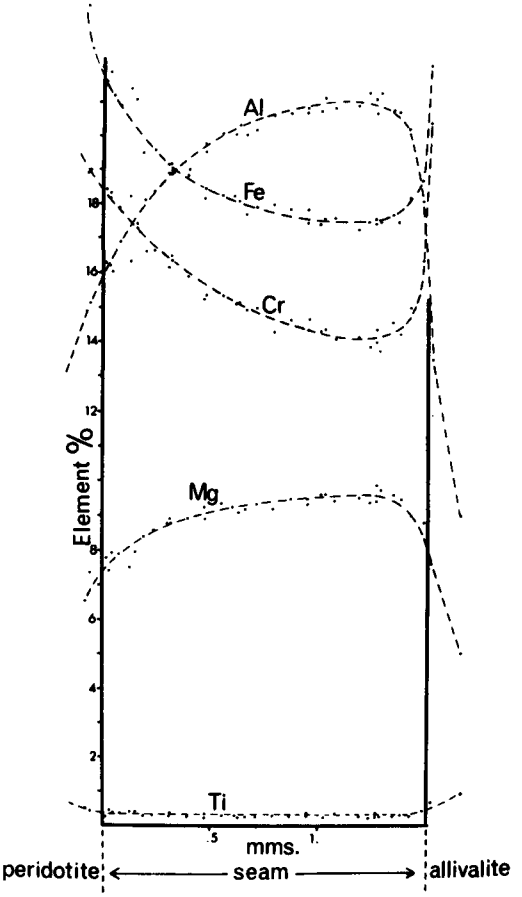

FIG. 2. Variation in chrome spinel compositions across the seam in R59. The top of the seam lies on the left.

the fact that within the peridotite the oxygen fugacity is buffered by the reaction olivine $\rightleftharpoons$ pyroxene + magnetite (Putnis, 1979) whereas in the allivalite the spinels are usually isolated from any iron-bearing phase. This investigation confirms that in such a chemically heterogeneous system significant variation in oxygen fugacity may persist on a small scale. Thus a sampling of spinel grains from a single thin section taken across a seam provides specimens of different compositions which have existed under different f_{O_2} conditions.

In this paper we describe the oxidation effects observed in two specimens: R117 taken from the junction of the unit 13 allivalite with the unit 14 peridotite, and R59 from the junction of the unit 7 allivalite with the unit 8 peridotite. (Units as defined by Brown, 1956. Specimens collected by P. Henderson, British Museum (Natural History).) The spinel analyses were carried out using an energy-dispersive electron microprobe and the oxidation products were characterized by transmission electron microscopy, selected area diffraction, and microanalysis facilities fitted to a Philips 400 transmission electron microscope.

Chrome spinel compositions. Electron microprobe analyses were made of chrome spinels lying in four different local environments in and around both seams: chrome spinel grains totally enclosed by olivine in the peridotite layers; chrome spinel grains within embayments in olivine in the peridotite layers; chrome spinel grains within the seams; and chrome spinel grains within the allivalite and totally enclosed by plagioclase feldspar. A further description of these environments in terms of the petrography of the rocks has been given by Henderson (1975).

The most striking feature of these analyses is the compositional difference between seam and non-seam chrome spinels, and secondly the systematic variation in the composition of seam spinels as a function of their position in the seam (figs. 1, 2). The seam spinels are very markedly depleted in iron

and chromium and enriched in aluminium and magnesium compared with chrome spinels lying outside the seam. The titanium content is also slightly lower in the seam spinels.

The chrome spinels that lie outside the seams have none of the obvious systematic compositional variations shown by the seam spinels. Their composition is apparently dependent on the nature of the adjacent phases and on the extent of any reaction between them. Generally, however, spinels totally enclosed by olivine have lower magnesium and aluminium contents and higher chromium contents than those that lie in embayments and show a reaction relationship with the olivine. Spinels totally enclosed by feldspar in the allivalite layer have the lowest magnesium and aluminium contents and the highest titanium contents. Some typical chrome spinel analyses from these environments are given in Table I.

It is not the purpose of this paper to speculate on the nature of the post-cumulus reactions that have partly or wholly contributed to these chemical variations. Here we are merely using the bulk composition of the spinels as one aspect of the characterization of their oxidation behaviour.

TABLE I. *Chrome spinel analyses from samples R117 and R59*

Element %	1	2	3	4	5	6
Mg	2.46	7.74	9.31	8.73	8.62	5.10
Al	4.34	18.64	21.04	19.92	18.00	12.15
Ti	2.14	0.49	0.33	0.39	0.41	0.56
Cr	16.42	15.77	13.38	14.50	16.04	18.40
Mn	0.30	0.26	0.15	0.27	0.25	0.33
Fe	43.49	21.91	18.93	21.19	20.60	30.13
Co	0.43	0.27	0.34	0.14	0.34	0.38
Ni	0.17	0.17	0.14	0.16	0.14	0.12
Element %	7	8	9	10	11	12
Mg	6.39	7.51	9.23	9.43	8.62	5.56
Al	11.52	16.32	19.71	21.24	17.61	11.30
Ti	1.34	0.38	0.30	0.26	0.36	0.73
Cr	20.67	18.33	15.34	13.93	17.71	22.39
Mn	0.13	0.25	0.21	0.20	0.15	0.32
Fe	26.74	21.91	18.19	17.55	20.87	27.98
Ni	0.12	0.12	0.23	0.16	0.18	0.12

Bulk chrome spinel analyses are presented in element weight percentages as the presence of a significant amount of very fine ilmenite exsolution lamellae means that spinel stoichiometry cannot be assumed.

Key to chrome spinel environments:

1. Within the allivalite (R117).
2, 3, 4. Within the seam at the base, middle and top respectively (R117).
5. Within an embayment in olivine in the peridotite (R117).
6. Totally enclosed by olivine in the peridotite (R117).
7–12. Are from R59 in similar environments to 1–6 respectively.

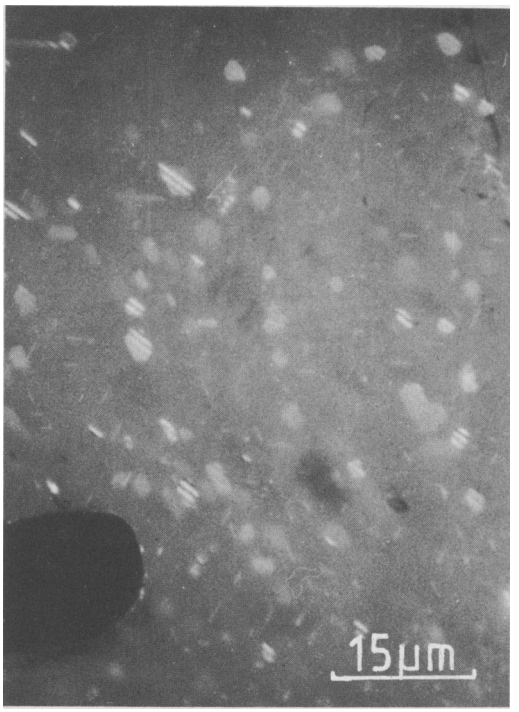

FIG. 3. Oil immersion reflected light micrograph of a chrome spinel grain showing a high density of platelet-like inclusions.

Reflected light microscopy

At high magnifications (× 1400) oil immersion reflected light microscopy revealed that most of the chrome spinel grains contained a high density of very fine well-oriented platelets of an exsolved phase. These could be observed by the interference fringes formed when the platelets were inclined to the surface of the grain (fig. 3). In some grains the platelets were large enough to be identified as anisotropic with a reflectivity higher than that of the spinel and hence were assumed to be of a rhombohedral phase. Electron microprobe analysis did not reveal any significant variation in composition in different parts of the same grain. As the distribution of the platelets was different in the two specimens examined they will be described in turn:

Specimen R117. Chrome spinel grains within the allivalite immediately below the seam almost invariably contain exsolution lamellae, which at times are coarse enough to be observed with a lower power objective. These spinel grains have a typical composition similar to analysis 1 in Table I.

Chrome spinel grains lying within the seam show an abrupt decrease in the scale of the exsolution lamellae. The platelets are only just within the

resolution of the high power objective. Their distribution is uniform throughout the grain and there is no evidence for any preferred nucleation on grain boundaries and cracks. The most striking feature of the distribution of the exsolved platelets is that in this seam they only occur in chrome spinels in the lower part of the seam. An abrupt boundary about 3.5 mms from the allivalite/seam junction defines a cut-off line above which no exsolution lamellae could be found. This boundary does not appear to correspond with any significant change in the bulk composition of the spinels (fig. 1). It does approximately correspond, however, to the region where olivine becomes a major constituent within the spinel-rich seam.

Small grains of interstitial chalcopyrite and pyrite occur throughout the seam. Where the sulphide is in contact with a precipitate-bearing spinel it is noticeable that a precipitate-free zone often occurs in that part of the spinel grain adjacent to the sulphide.

Chrome spinel grains within the peridotite overlying the seam do not contain any exsolved phases. The olivine, however, does show the effects of oxidation with the formation of eutectoid-like intergrowths of magnetite + pyroxene lying within lamellae in the olivine (Putnis, 1979).

Specimen R59. In this specimen, in which the seam is 1.5 mm thick (fig. 2) exsolved platelets were found in almost all of the chrome spinel grains examined. Within the allivalite the chrome spinel has coarser and more widely spaced lamellae compared to the seam spinels in which the lamellae are again very fine and densely distributed. In this case there is a noticeable tendency for the platelets to be concentrated towards the centre of the grains with a precipitate-free zone around the edges. Very fine late-stage blebs of sulphide occur throughout the seam and often form coatings around the chrome spinel grains.

The chrome spinels that lie in the peridotite above the seam, either in embayments or totally enclosed by olivine also contain exsolved platelets. This is in contrast to the situation found in Specimen R117. In the totally enclosed spinels within the olivine, the platelets are coarser and more widely spaced with a distribution very similar to those in the spinels in the allivalite.

Electron microscopy, diffraction, and microanalysis

Transmission electron microscopy of ion-beam thinned chrome-spinel grains was used to characterize the exsolved platelets. Most of the platelets encountered in the thinned specimens were less than about 0.1 μm thick and 0.5 μm long. Their composition was semiquantitatively determined by analytical electron microscopy, using an EDAX attachment fitted to a Philips EM 400 electron microscope. The techniques used were similar to those described by Cliff and Lorimer (1975). Analyses were made of the platelets and of the matrix on either side. The concentration ratios at each point were obtained by using the relation $I_1/I_2 = kC_1/C_2$, where I_1 and I_2 are the measured characteristic X-ray intensities, C_1 and C_2 are the weight fractions of the two elements in question and k is a proportionality factor. The proportionality factor was determined by measuring integrated peak intensities from a set of thin standards (Price, unpublished). The results indicate that the platelets are very greatly enriched in titanium relative to the matrix. Iron and magnesium are also present in the approximate ratios Fe:Ti = 2:3 and Mg:Ti = 1:6. On this basis the composition of the platelets approximates to that of a magnesium bearing ilmenite, similar to that found in oxidized chromites by Bøe (1978).

Observations of their orientations and diffraction patterns indicates that the spinel contains platelets of two distinctly different phases. One set of platelets lies on the {111} planes of the spinel matrix and produces a diffraction pattern that can be indexed on a rhombohedral unit cell indicative of an R_2O_3 sesquioxide phase. The platelets have a hexagonal outline and the interface with the spinel matrix is bounded by dislocations (fig. 4). The

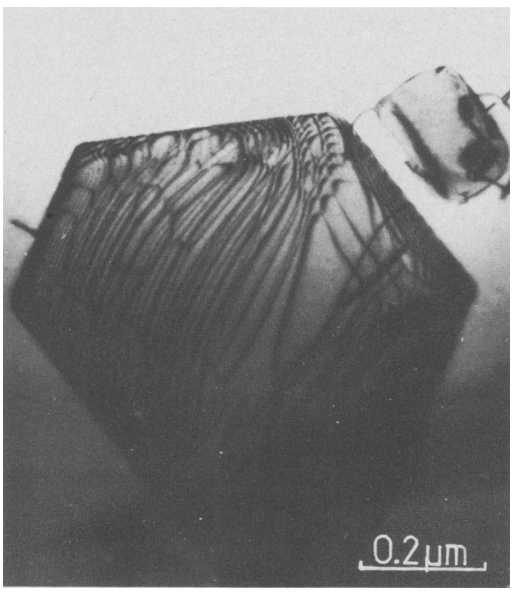

FIG. 4. Transmission electron micrograph approximately normal to the c axis of the rhombohedral phase, showing the dislocations at the interface with the spinel matrix.

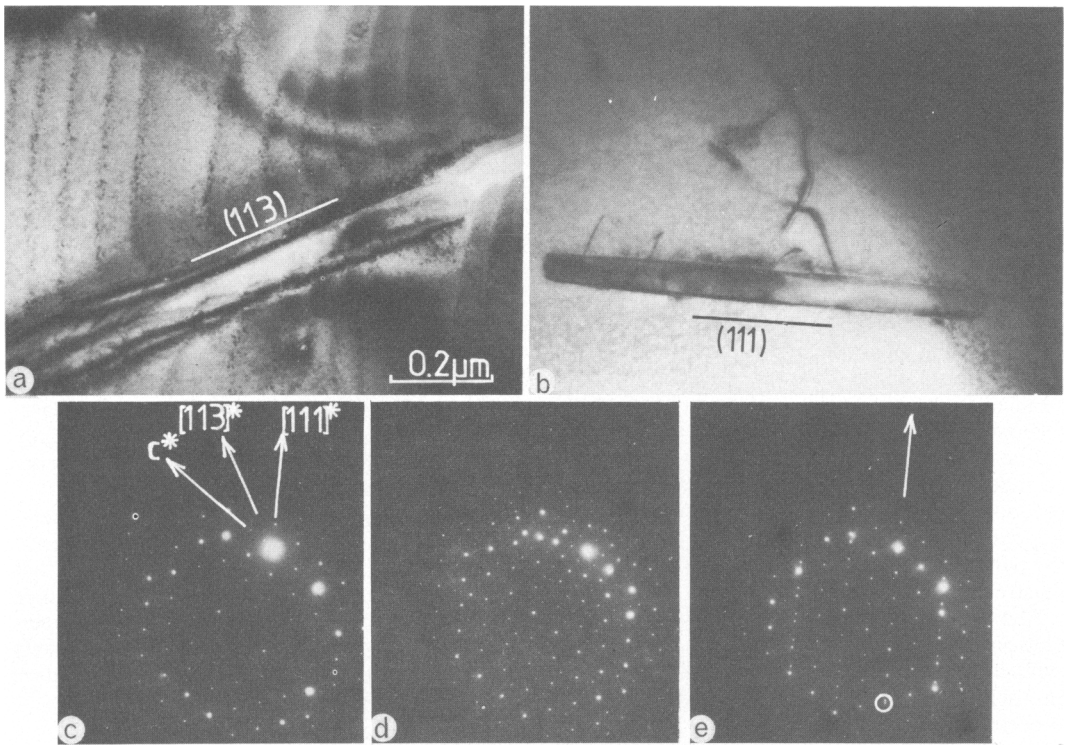

FIG. 5. Transmission electron micrographs and oriented diffraction patterns from the two exsolved phases in a single chrome spinel grain: (*a*) the intermediate phase platelet lying on (113) planes of the spinel matrix. The structure in the matrix is partly due to the ion-beam thinning process: (*b*) a platelet of the rhombohedral phase lying on (111) planes of the spinel matrix; (*c*) an oriented electron diffraction pattern from the spinel matrix; (*d*) an electron diffraction pattern taken over the platelet in (*a*) showing the spinel superstructure. No splitting on reflections is evident; (*e*) an electron diffraction pattern taken over the platelet in (*b*) showing the overlapping patterns from the spinel and the rhombohedral phases. The arrow is the direction common to the *c* axis of the rhombohedral phase and the [111] direction of the spinel. The circled split reflections show the degree of misfit between the phases in this direction.

diffraction data and the analyses indicate that the hexagonal platelets are magnesian ilmenite. The second set of platelets lies on {113} planes of the matrix and the diffraction pattern can be indexed on a unit cell which is a superstructure of the spinel structure. Figs. 5*a*, *b* are electron micrographs of platelets of the two phases within a single grain of chrome spinel while figs. 5*c*, *d*, *e* show the oriented diffraction patterns of the spinel matrix alone, matrix + superstructure spinel phase, and matrix + rhombohedral phase respectively.

The analyses and observations indicate that the bulk composition of the chrome spinel grains must lie on the cation-deficient side of the AB_2O_4 spinel stoichiometry. Such deviations from stoichiometry could occur at high temperatures (*c.* 1000 °C) where a certain degree of solid solution exists between a spinel and a sesquioxide phase (Greskovitch and Stubican, 1968), or alternatively at lower temperatures by the oxidation of a stoichiometric spinel phase. In the present case it is considered that the former is unlikely. Slow cooling from the high temperatures involved would not produce the fine scale and distribution of the platelets observed. A homogeneous distribution of fine platelets with no observable nucleation on grain boundaries, cracks, etc. suggests a relatively low temperature process. The presence of the superstructure spinel phase also suggests a lower temperature origin, a point that will be taken up in the next section. We conclude that the platelets of both phases form as a result of oxidation processes and that the variation in their distribution arises from local variations in oxygen fugacity, as well as bulk chemistry.

The spinel superstructure phase

A large number of electron diffraction patterns that include both the platelets of the superstructure phase and the matrix were analysed to determine uniquely both the orientation of the platelets and the unit cell of the superstructure phase. These composite diffraction patterns, such as that in fig. 5*d* show no splitting of the subcell reflections indicating very little mismatch between the matrix and the superstructure phase. There is no evidence for dislocations at the interface, suggesting that it may be coherent, although no lattice imaging has been carried out to confirm this. Compared with the rhombohedral phase, however, which shows both an incoherent interface and splitting of the subcell reflections (figs. 4, 5*e*), the mismatch is small.

The unit cell of the superstructure phase could be indexed on a body-centred orthorhombic (or pseudo-orthorhombic) cell with lattice parameters $a/\sqrt{2} \times a \times 3a/\sqrt{2}$ (where a is the cell parameter of the parent spinel structure). This superstructure is illustrated in fig. 6.

The formation of such spinel superstructure phases has been well documented in a number of synthetic systems in which the exsolution of a rhombohedral sesquioxide phase is the equilibrium process (Greskovitch and Stubican, 1968; Lewis, 1969; Dekker and Rieck, 1974). In each of these cases the exsolved products were derived from a high-temperature spinel solid solution and the superstructures found were different from that described here. Essentially, the spinel superstructure is a metastable intermediate phase that forms under non-equilibrium conditions when the formation of the stable rhombohedral phase is kinetically impeded. The nucleation of the rhombohedral phase involves a change in the oxygen close-packing from cubic to hexagonal and hence a relatively high activation energy is implied. At lower temperatures such a process will be kinetically difficult and the non-stoichiometric spinel may reduce its free energy by an alternative process. Segregation of oxidation defects such as vacancies and Fe^{3+} centres, followed by vacancy ordering, is such an alternative and results in a spinel superstructure. The oxygen close-packing is essentially unaltered and consequently the activation energy for nucleation will be lower.

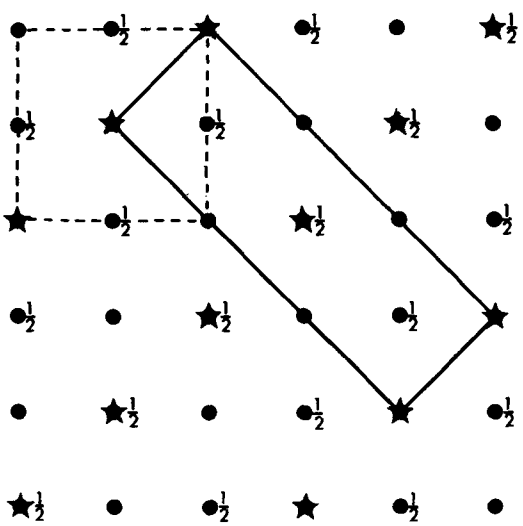

FIG. 6. The relationship between the unit cell of the spinel structure (dashed lines) and the unit cell of the intermediate phase (full lines). The black dots represent lattice points of the face-centred spinel structure, while the starred dots are lattice points in the body-centred intermediate structure only.

Under non-equilibrium conditions the metastable phase or phases that form are governed largely by the kinetics of the process. It is not surprising therefore that in systems of the type AB_2O_4–R_2O_3 a large number of different superstructure phases have been found and it is likely that both the stoichiometry and the temperature will affect the nature of the phase formed.

The formation of such intermediate phases is a common characteristic of processes in a number of mineral systems where the nucleation of a structurally dissimilar phase is involved. In each case the intermediate phase has a structure that is a variant of the parent structure. This has been found to be the case in the oxidation of olivine (Putnis, 1979) and in the exsolution of hematite from rutile (Putnis, 1978). An intermediate phase very similar to that described here has also been recently found in oxidized ceylonites where the equilibrium product is corundum (Price and Putnis, 1979).

The cation:anion ratio in the intermediate phase described here could not be determined from the microanalyses. Some estimate can be made, however, by considering the possible number of vacancies in the body-centred orthorhombic cell. As the increase in unit-cell volume is due to the presence of these vacancies we may associate either one of two vacancies with each lattice point. In other words the orthorhombic unit cell may contain either two or four vacancies. (Note that these vacancies are the extra vacant sites not already present in the stoichiometric spinel structure.)

The spinel unit cell contains 24 cations and 32 oxygen atoms. As the unit-cell volume of the intermediate phase is $1\frac{1}{2}$ times that of spinel the cell content may be 34 cations to 48 anions (if there are two extra vacancies) or 32 to 48 (with four extra vacancies). This should be compared with the

rhombohedral phase where a similar volume would have a cation:anion ratio of 32:48. Generally intermediate phases have a composition between that of the parent phase and the stable product, and as the ratio 34:48 lies half-way between that of spinel and the rhombohedral phase it is suggested that this may be a likely composition. The cation content of the intermediate phase could not be determined but we assume that it lies between that of the spinel and the magnesian ilmenite.

Discussion

The first point that emerges from the observations made here is that despite the very low proportion of the ulvöspinel component in the spinels the oxidation product is a magnesian ilmenite. The wide variations in the bulk chemistry do not appear to affect this result. It has been shown by Buddington and Lindsley (1964) that the addition of a small amount of ulvöspinel component to magnetite very significantly reduces the equilibrium fugacity for oxidation, especially at low temperatures, and that the rhombohedral phase formed is very highly enriched in titanium. Although the addition of other components will doubtlessly modify the equilibrium f_{O_2} values, the overall result remains the same. This high preferential partitioning of Ti into the rhombohedral phase dominates the oxidation behaviour of Ti-bearing spinels even when the ulvöspinel content is less than 1%. In practice this means that the first-formed equilibrium oxidation product will be a phase in the $FeTiO_3$–$MgTiO_3$ solid solution.

When all of the titanium is in a rhombohedral phase the remaining spinel composition lies in the system $(Fe,Mg)Al_2O_4$–$(Fe,Mg)Cr_2O_4$–Fe_3O_4. Turnock and Eugster (1962) have demonstrated that corundum + magnetite result as the products of oxidation of hercynite and that the oxidation of the magnetite component to hematite requires higher oxygen fugacities. Therefore with increasing oxygen fugacity the oxidation sequence in Ti-bearing spinels would be ilmenite–corundum–hematite. The formation of hematite and Cr_2O_3 products requires high values of f_{O_2} (Katsura and Muan, 1964) and is unlikely to be important in this system. In the Rhum chrome spinels the oxygen fugacity evidently did not reach the values required for the formation of corundum.

The presence of an intermediate spinel superstructure phase indicates relatively low-temperature oxidation and this conclusion is supported by the fine scale and homogeneous distribution of the platelets. Some guide to the oxidation temperature is provided by data on the oxidation of titanomagnetite. The direct formation of ilmenite from titanomagnetite oxidation occurs above 600 °C (Lindsley, 1962) while below this temperature metastable cation deficient spinels of the titanomaghemite series are formed (Verhoogen, 1962). In the Rhum chrome spinels both the stable and metastable products are present, suggesting that oxidation occurred over a temperature range during subsolidus cooling with the metastable phase being formed at lower temperatures.

The variation in oxygen fugacity in and adjacent to the chrome spinel seams is evidenced by the distribution of oxidized and unoxidized spinel grains. In this respect the two seams examined differed and will be briefly discussed in turn.

R117. Only spinel grains in the lower part of the seam and within the allivalite are oxidized, although no correlations with composition could be made. Spinel grains within the allivalite (analysis 1) show relatively coarse ilmenite lamellae, whereas grains lying within the peridotite immediately above the seam are unoxidized, despite containing more Ti (analysis 6) than oxidized grains within the seam (analysis 3). It appears that within the peridotite and the upper part of the seam the oxygen fugacity is buffered by the oxidation of the olivine (Fo_{86}), which shows fine magnetite–pyroxene intergrowths (Putnis, 1979). This creates an oxygen-fugacity gradient across the seam with the fugacity increasing towards the allivalite boundary. At some point within the seam the f_{O_2} reaches the equilibrium value for the oxidation of the chrome spinel. As noted earlier this value appears to depend on the titanium content rather than the bulk composition.

At a later stage in the cooling history the f_{O_2} decreased sufficiently for the formation of interstitial sulphides. A zone in the spinel grains adjacent to these sulphides is free of any oxidation products and provides some evidence for the re-equilibration of the spinel, apparently by resorption of the ilmenite platelets.

R59. This specimen differs from R117 in that all of the spinel grains show evidence of oxidation, including those within and adjacent to the olivine. The scale of the platelets depends on the bulk titanium content and the immediate environment appears to have no effect. The olivine shows no signs of oxidation. Thus in this case the equilibrium f_{O_2} value for the oxidation of the chrome spinel is lower than that for the oxidation of the olivine, a fact that must be dependent on their compositions. The olivine composition is Fo_{87} and hence not significantly different from that in the peridotite of specimen R117. The titanium content of the spinel is somewhat higher (cf. analyses 6 and 12) although with such small overall values and the variations between grains no clear conclusions can be drawn.

Nevertheless at low temperatures the equilibrium oxygen fugacity for ulvöspinel oxidation is very dependent on Ti content (Buddington and Lindsley, 1964) and the relevant f_{O_2} values for oxidation of olivine and chrome spinel are unlikely to be very different. It could be concluded therefore that in the case of R59 slight compositional differences favoured the oxidation of the chrome spinel with respect to the oxidation of the olivine.

Late stage reduction of f_{O_2} again produced interstitial sulphides throughout the seam and in this case re-equilibration of the spinels is more obvious. Spinel grains are frequently rimmed with thin sulphide coatings and a platelet-free zone about 0.01 mm wide is formed within the spinel. This represents a diffusion distance over which reduction and consequently resorption of the platelets was possible.

Conclusions

Local variations in oxygen fugacity associated with layering in the Rhum Ultramafic complex have led to significant differences in the extent of oxidation of the chrome spinel seams. Oxidation occurred at moderate to low temperatures (*c.* 600 °C) producing a fine-scale homogeneous distribution of ilmenite platelets as well as platelets of a newly described intermediate phase. The nature and scale of the platelets is highly dependent on Ti content and an Mg-ilmenite is the first-formed oxidation product even in spinels with a TiO_2 content of less than 1 %.

Acknowledgements. We would like to thank P. Henderson (British Museum, Natural History) for providing the specimens from Rhum, and the Natural Environment Research Council for financial support. Analytical electron microscope facilities were provided by Dr M. Stobbs, Department of Metallurgy and Materials Science, Cambridge University.

REFERENCES

Bøe (P.), 1978. *Can. Mineral.* **16,** 597–600.
Brown (G. M.), 1956. *Phil. Trans. Roy. Soc.* **B, 240,** 1–53.
Buddington (A. F.) and Lindsley (D. H.), 1964. *J. Petrol.* **5,** 310–57.
Dekker (E. H. L.) and Rieck (G. D.), 1974. *Rev. Int. Hautes Temp. Refract.* **11,** 187–92.
Greskovitch (C.) and Stubican (V. S.), 1968. *J. Am. Ceram. Soc.* **51,** 42–6.
Henderson (P.), 1975. *Geochim. Cosmochim. Acta,* **39,** 1035–44.
—— and Suddaby (P.), 1971. *Contrib. Mineral. Petrol.* **33,** 21–31.
Katsura (T.) and Muan (A.), 1964. *Trans. Am. Inst. Min. Metal. Eng.* **230,** 77–84.
Lewis (M. H.), 1969. *Phil. Mag.* **20,** 985–98.
Lindsley (D. H.), 1962. *Carnegie Inst. Washington Yearb.* **61,** 100–6.
—— 1976. In: *Oxide Minerals Short Course Notes.* Min. Soc. Am.
Lorimer (G. W.) and Cliff (G.), 1976. In: Wenk (H. U.), ed. *Electron Microscopy in Mineralogy.* Ch. 7.3. Springer-Verlag, Heidelberg.
Price (G. D.) and Putnis (A.), 1979. *Contrib. Mineral. Petrol.* **69,** 355–9.
Putnis (A.), 1978. *Phys. Chem. Minerals,* **3,** 183–97.
—— 1979. *Mineral. Mag.* **43,** 293–6.
Turnock (A. C.) and Eugster (H. P.), 1962. *J. Petrol.* **3,** 533–65.
Verhoogen (J.), 1962. *J. Geol.* **70,** 168–81.

[*Manuscript received 23 April 1979*]